Available online at www.sciencedirect.com

ScienceDirect

Acta Materialia 65 (2014) 373–382

Acta MATERIALIA

www.elsevier.com/locate/actamat

Correlation between defect structure and electrochemical properties of mixed conducting $La_{0.1}Sr_{0.9}Co_{0.8}Fe_{0.2}O_{3-\delta}$

Moon-Bong Choi [a], Sang-Yun Jeon [a], Bhupendra Singh [a,b], Young-Sung Yoo [c],
Jin-Ha Hwang [d], Sun-Ju Song [a,b,*]

[a] *Ionics Lab, School of Materials Science and Engineering, Chonnam National University, 300 Yongbong-dong, Buk-gu, Gwang-Ju 500-757, Republic of Korea*
[b] *Research Institute for Catalysis, Chonnam National University, Gwang-Ju 500-757, Republic of Korea*
[c] *Green Growth Technology Laboratory, Korea Electric Power Research Institute, 65 Munji-Ro, Yuseong-Gu, Daejeon 305-760, Republic of Korea*
[d] *Department of Materials Science and Engineering, Hongik University, 72-1 Sangsu-dong, Mapo-gu, Seoul 121-791, Republic of Korea*

Received 5 August 2013; received in revised form 3 November 2013; accepted 4 November 2013
Available online 27 November 2013

Abstract

The high catalytic properties of LSCF1982 arise from its defect structure. In this work, the oxygen nonstoichiometry (δ) of LSCF1982 was analyzed as a function of oxygen partial pressure (P_{O_2}) and temperature for the $-6 \leqslant \log(P_{O_2}/\text{atm}) \leqslant 0$ and $800 \leqslant T/°C \leqslant 1000$ ranges. A defect structure model for LSCF1982 was presented, which fitted well with the experimental data for δ. The equilibrium constants of appropriate defect reactions were determined. Analysis of the defect structure of LSCF1982 suggested that the conduction mechanism of LSCF1982 is governed by hopping conduction and band conduction of p-type carriers, which was determined by the analysis of thermoelectric power. The characteristic membrane thickness (L_c), indicating the transition from predominantly bulk-diffusion controlled reaction to surface-exchange controlled reaction, had a value of $3.5 \pm 0.9 \times 10^{-2}$ cm. The oxygen vacancy diffusivity was calculated from the relationship between oxygen flux and oxygen chemical potential gradient. The chemical expansion was measured as a function of P_{O_2} and temperature in the $10^{-3} \leqslant P_{O_2}/\text{atm} \leqslant 0.21$ and $800 \leqslant T/°C \leqslant 1000$ ranges. The chemical expansion model based on the relative change in mean ionic radius was employed to compute the chemical expansion vs. δ, which indicated that the spin states of B-site transition metal ions are a mixture of high-spin and low-spin states, and made the transition from the low-spin to the high-spin state with an increase in δ and temperature.

Keywords: Defect; Oxygen nonstoichiometry; Diffusion; Fuel cell material; Mixed conductor

1. Introduction

Mixed ionic–electronic conductor (MIEC) oxides have many potential applications—e.g. separation membranes for high-purity oxygen production, surface catalysts or reactors for the partial oxidation of methane to syngas, and electrodes in fuel cells and batteries—mainly due their higher ionic and electronic conductivity. Among various MIEC oxides with perovskite-type structure, the oxides of $La_{1-x}Sr_xCo_{1-y}Fe_yO_{3-\delta}$ (LSCF) series have been extensively studied for such applications [1–8]. LSCF perovskite oxides possess good electronic conductivity at intermediate temperatures and high oxygen surface-exchange and bulk-diffusion characteristics, and good catalytic activity [9,10]. Among the LSCF series, $La_{0.1}Sr_{0.9}Co_{0.8}Fe_{0.2}O_{3-\delta}$ (LSCF1982) shows a high electrical conductivity and high oxygen diffusivity [11–13]. Generally, this higher electrochemical performance is simultaneously controlled by the nature and composition of A- and B-site cation species, temperature and P_{O_2}. The substitution of Sr^{2+} by La^{3+} is charge compensated by the reduction of B-site transition

---

[*] Corresponding author at: Ionics Lab, School of Materials Science and Engineering, Chonnam National University, 300 Yongbong-dong, Buk-gu, Gwang-Ju 500-757, Republic of Korea. Tel.: +82 62 530 1706; fax: +82 62 530 1699.
E-mail address: song@chonnam.ac.kr (S.-J. Song).

1359-6454/$36.00 © 2013 Acta Materialia Inc. Published by Elsevier Ltd. All rights reserved.
http://dx.doi.org/10.1016/j.actamat.2013.11.006

metal ion and filling of oxygen vacancies ($V_O^{\bullet\bullet}$). The B-site substitution of Co with Fe improves the chemical stability of the structure towards reducing atmospheres [11,14,15]. Clearly, the nature and composition of species at the A- and B-sites influence the defect structure, which in turn affects the physicochemical properties. Therefore, the analysis of defect structure is very important, because several transport properties of oxide are directly connected with defect structure in a given thermodynamic condition.

Previously, we have investigated LSCF for a number of applications [1,3,5,16]. For further improvements in the practical applications of LSCF, however, it is necessary to investigate its fundamental thermodynamic and kinetic properties. For this purpose, we have previously reported some of these properties of LSCF1982, such as total conductivity, ionic conductivity, oxygen permeability, chemical expansion and oxygen nonstoichiometry as a function of temperature and P_{O_2} [17,18]. Since these fundamental thermodynamic and kinetic properties are dependent upon the concentration and nature of defect species present in the system, it is imperative to perform defect chemical analysis of LSCF1982 to obtain a better understanding of these properties. In this work, we present the defect structure model for LSCF1982 and analyze some of its fundamental properties in terms of the relationship among its structural elements.

2. Experimental

2.1. Synthesis of LSCF1982 and sample preparation

LSCF1982 powder was synthesized by the solid-state reaction method. La_2O_3 (Aldrich, 99.9%), $SrCO_3$ (Aldrich, 99.9%), Co_3O_4 (Aldrich, 99.9%) and Fe_2O_3 (Aldrich, 99.99%) were used as the starting materials. Stoichiometric amounts of the various oxide components required for LSCF1982 were mixed in a ball mill and the mixture was calcined at 1000 °C in air for 10 h. The as-calcined powder was ground and then was planetary ball-milled at 320 rpm for 2.5 h to obtain LSCF1982 powder with particle size of 1–3 μm [17]. Portions of the LSCF1982 powder were molded into pellets, which were then cold isostatically pressed at 150 MPa. The green pallets were sintered at 1200 °C in air for 10 h, and were then cut and polished.

2.2. Oxygen nonstoichiometry

The oxygen nonstoichiometry of LSCF1982 was measured as a function of oxygen partial pressure and temperature in the ranges $-6 \leqslant \log(P_{O_2}/\text{atm}) \leqslant 0$ and $800 \leqslant T/°\text{C} \leqslant 1000$, respectively, by the electrochemical coulometric titration method as described elsewhere [18–20]. The absolute value of oxygen nonstoichiometry was determined by the thermogravimetric full reduction method with a Cahn D-200 microbalance [21].

Table 1
The best-estimated fitting parameters for Eq. (10).

T (°C)	K_i (mol^2)	K_{re} (mol^2 atm$^{1/2}$)	K_a (mol^{-1})	K_B (mol)
1000	6.01×10^{-7}	1.11×10^{-9}	0	2.57×10^{-4}
950	1.13×10^{-6}	8.84×10^{-10}	0	6.19×10^{-4}
900	2.02×10^{-6}	2.78×10^{-10}	0	1.11×10^{-3}
850	5.15×10^{-6}	6.72×10^{-11}	8.35×10^{-2}	2.06×10^{-3}

2.3. Conductivity and thermopower

The total conductivity of LSCF1982 was measured by the four-probe DC method, as previously reported [17]. The thermopower (θ) was measured using a rectangular bar-type specimen (95% of theoretical density, $1.5 \times 1.5 \times 15\ \text{mm}^3$) by the steady-state method [22,23]. The experimental setup for the thermopower measurement is shown in Fig. 1. The rectangular specimen (①) was heated in the laboratory-made apparatus which consisted of a Pt-microheater (②), an alumina sample holder (③, ④), an S-type thermocouple (⑤) and a Pt-electronic probe (⑥). The Pt-microheater was used to generate a temperature gradient across the specimen. Two S-type thermocouples were used to measure the temperature difference between two ends of the specimen. The thermal voltage (E_{therm}), as a function of temperature difference ($2 \leqslant \Delta T/°\text{C} \leqslant 10$) between two ends of the specimen, was measured using the Pt-electronic probe (⑥). The Seebeck coefficient of the specimen was determined from the slope of the E_{therm} vs. temperature difference plot after compensating for the thermopower of the Pt-wire as earlier reported [22–24]. The overall measurements were conducted over the temperature and pressure ranges of $700 \leqslant T/°\text{C} \leqslant 1000$ and $10^{-3} \leqslant (P_{O_2}/\text{atm}) \leqslant 0.21$. P_{O_2} was maintained by flowing air and nitrogen gas mixture, which was monitored using an ex situ yttria-stabilized zirconia (YSZ) electrochemical sensor.

2.4. Oxygen permeability

The oxygen permeability was measured using dense LSCF1982 disks (theoretical density ~95%; diameter = 20 mm; thickness = 0.8, 1.0, 1.5, 2.3 or 2.7 mm). The disk surface was polished with 100-grit SiC paper to maximize the surface area for diffusion-controlled

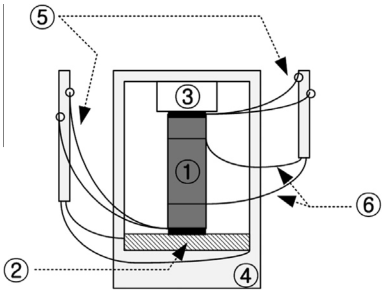

Fig. 1. Schematic of the thermoelectric power measurement setup: (1) specimen; (2) microheater; (3) alumina rod; (4) alumina sample holder; (5) S-type thermocouple; (6) EMF lead wire.